Measurements of coupled Rayleigh wave propagation in an elastic plate

Boon Wee Ti and William D. O'Brien, Jr., Electrical and Computer Engineering
John G. Harris, Theoretical and Applied Mechanics
University of Illinois at Urbana-Champaign
Urbana, IL 61801

Abstract

At frequencies where the thickness of an elastic plate is more than a wavelength thick, the propagation of the two lowest Rayleigh-Lamb modes in an elastic plate can be viewed as the propagation of a Rayleigh surface wave over two weakly coupled, surface-wave waveguides. That is, a Rayleigh wave launched on one surface gradually transfers to the other and then back. It does so in a length we call the beatlength. Measurements of the beatlength for brass plates are reported as a function of frequency and thickness. This phenomenon is readily excited and persists over a wide range of thicknesses and frequencies.

PACS numbers: 43.35Pt, 43.35Zc, 43.20Mv.

INTRODUCTION

The two lowest waveguide modes of an elastic plate can be described as the propagation of a Rayleigh surface wave that starts on one surface, but that gradually transfers to the other surface. It then transfers back to the surface from which it started, the whole cycle taking place over a distance we call the beatlength. Provided the product of wave number and thickness is sufficiently large, one can thus view a plate as two weakly coupled, surface-wave waveguides. The objective of this letter is to report measurements of the beatlength in brass plates. This may be one of the first detailed experimental assessments of this phenomenon, though its possibility has been noted by Auld[1], Viktorov[2] and Brekhovskikh and Goncharov[3]. Moreover, Li and Thompson[4] made similar measurements, but did not widely report them.

The longer service life of structures such as pipelines means that they must be monitored more thoroughly, and over a longer period of time, for damage. Using coupled surface waves may be one way to inspect the inner, and therefore not easily accessible, surface of a pipe from its outer surface. Moreover, if the damage were a small surface-breaking fatigue crack, then a surface wave would readily detect the crack because the surface wave would strike the crack broadside, or if the damage were corrosion, then a surface wave would be more severely attenuated by the patch of corrosion at the surface than a bulk wave. The present measurements indicate that the coupled surface waves are readily excited and detected so that they can be used for such nondestructive testing.

The basic idea is presented graphically. Figure 1 shows the dispersion relation for the two lowest, Rayleigh-Lamb modes. The lower curve is that for the lowest antisymmetric mode , while the upper curve is for the lowest symmetric mode. The vertical axis is the normalized angular frequency (ω multiplied by (h/c_t), where h is one half the thickness of the plate and c_t is the transverse wave speed). The horizontal axis is the normalized wave number (β multiplied by h). The short dashed line indicates the straight line formed by $\omega h/c_t$ plotted against $\beta_r h$, where β_r is the Rayleigh wave number. The slope is (c_r/c_t), where c_r is the Rayleigh wave speed. In the neighborhood of the intersection points of the long dashed horizontal line with the dispersion curves, the x

particle displacements look roughly as sketched in Fig. 2. Figure 2(a) sketches the symmetric mode, Fig. 2(b) the antisymmetric mode and Fig. 2(c) their algebraic sum. If the symmetric and antisymmetric modes are both excited in phase, then the sum approximates a Rayleigh wave on the upper surface. This is indicated by the solid line in Fig. 2(c). However, each mode propagates with a slightly different wave number, β_s for the symmetric mode and β_a for the antisymmetric mode. After a distance $L/2$, the two modes move π out of phase. Adding the two modes together at this location approximates a Rayleigh wave on the lower surface. This is indicated by the dashed line in Fig. 2(c). After propagating an additional distance $L/2$, the modes move back into phase (more accurately 2π out of phase) and their sum again approximates a Rayleigh wave, now on the upper surface. In this sense the propagation of the two modes can be viewed as a Rayleigh surface wave coupling from one surface-wave waveguide to another. Figure 1, by means of the vertical dashed lines, indicates the difference 2ε between the wave numbers β_s and β_a. The difference between β_s and β_r is almost equal to that between β_r and β_a. The beatlength L of the coupled waves is that distance over which the two modes move out of phase by 2π, that is,

$$(\beta_a - \beta_s)L = 2\pi \tag{1}$$

or

$$L/h = \pi/h\varepsilon \tag{2}$$

Brekhovskikh and Goncharov[3] give an estimate of ε for large βh. However, we use the exact, Rayleigh-Lamb dispersion relation[5] to calculate ε and L/h.

I MEASUREMENTS

The longitudinal and shear wave speeds in brass are experimentally determined using standard pulse-echo techniques with a Panametrics 5800 Pulser/Receiver. The longitudinal wave speed is found using a 15 MHz Panametrics V3619 immersion transducer. The shear wave speed is found using a 20 MHz Panametrics V222-BA-RM normal incidence shear-wave contact transducer.

The view, from above, of the experimental arrangement is sketched in Fig. 3. A focused 3 *MHz* Panametrics V3680 transducer directs a focused ultrasonic beam at the surface of a 2.38 *mm* thick brass plate at the Rayleigh angle θ_r.

The sound is coupled to the plate by a jacket of water that surrounds the sound beam, as shown in Fig. 3. The plate is otherwise in air, so that no substantial fluid-loading occurs.

The Rayleigh angle is experimentally determined as follows. The normal beam axis to the brass plate is found by adjusting the focused transducer to an angle where the reflection, measured using the pulse-echo mode, is maximum. Then the transducer is rotated to θ_r,which angle is calculated (see Section III) from the measured wave speeds. The rotation is computer controlled by a positioning system that has a linear accuracy of about 5 μm and a rotational accuracy of about 0.02°.

The beatlength is experimentally determined as follows. With the incident beam at the Rayleigh angle and the focus on the metal plate, the transmitter is moved parallel to the plate surface, toward the broadband receiver, a Deci Model SE 1025-H308 surface contact transducer. The transmitter is moved in 200 μm intervals, and at each interval, a 1024-point, 10 *MHz* data record of the temporal, received sinusoidal signal is recorded by the receiver. The RMS value for each position is calculated and recorded.

The transmitter is moved a distance slightly greater than 3 times the estimated beatlength. This corresponds to collecting 150 RMS values. The RMS values are Fourier transformed using a 4096 FFT. The power spectrum is calculated to determine the peak corresponding to the beatlength.

II RESULTS

The measured longitudinal wave speed in brass is 4536 *m/s*. The measured shear wave speed in brass is 2215 *m/s*. Their ratio is 2.048.

Figure 4 shows a typical measurement (case 4 of Table 1). Figure 4(a) shows the amplitude modulated signal from a 100 *mm* scan, that is, the transmitter was moved 100 *mm*, in 200 μm intervals, toward the receiver. Figure 4(b) shows the spatial power spectrum of the signal from Fig 4(a). The vertical line marks the theoretically predicted spatial beat frequency calculated using the exact, Rayleigh-Lamb dispersion relation[5].

Figure 5 plots L/h against $\omega h/c_t$. The error bars represent $\pm 10\%$ of a theoretically predicted value. The transmitter's operating frequency f is varied to produce the 7 different $\omega h/c_t$ cases.

Table 1 summarizes the results of the experiment conducted on brass. The wave number β must be greater than ε to produce a spatially modulated signal. Thus β/ε is tabulated. The theoretical value for L/h is calculated from the exact dispersion relations. The experimentally determined spatial beat frequency, beatlength and normalized beatlength are tabulated in the last three columns.

III DISCUSSION

The Rayleigh angle, θ_r is defined as

$$\theta_r = \sin^{-1}(c/c_r) \tag{3}$$

where c is the speed of sound in water. A very good approximation for c_r is[6]

$$c_r/c_t = (0.87 + 1.12\nu)/(1+\nu) \tag{4}$$

where

$$\nu = \left[(c_l / c_t)^2 - 2 \right] / 2 \left[(c_l / c_t)^2 - 1 \right] \tag{5}$$

From the measured values of c_l and c_t, $c_r = 2069$ *m/s* and $\theta_r = 47.58°$. This is the angle used in these measurements.

Figure 4 (b) suggests that the beat phenomenon is robust in the spatial frequency domain, and that the measured spatial frequency is in agreement with theory (see Table 1). Figure 5 indicates that the measured values of the spatial beat frequency lie close to or within ±10% of the theoretically predicted values. Brekovskikh and Goncharov[3] suggest that βh must be large for the coupling phenomena to be clearly observed and their estimate of ε assumes this. However, our values of βh ranged from 2 to 5 and yet we observe the coupling phenomena without difficulty. Moreover, the beatlengths indicate that the use of the coupled waves to access an inner surface is realistic. None of the beatlengths is so great that the signals would become too severely attenuated, with distance, to carry information from the far surface.

Initially, we had been concerned that, in addition to the two lowest modes, we might excite higher modes and as a consequence some power would be carried by them and lost to the coupling phenomenon. This appears not to be the case suggesting that when we are incident at the Rayleigh angle we strongly excite only the two lowest modes.

ACKNOWLEDGMENTS

The support of American Chemical Society (Petroleum Research Fund) Grant PRF 29555-AC9 for this work is gratefully acknowledged. Boon Wee Ti also thanks the Economic Development Board of Singapore for providing a scholarship to study at UIUC.

REFERENCES

[1] B.A. Auld, *Acoustic Fields and Waves in Solids*, Vol 2 (Krieger, Malabar, FL, 1990), pp.93-94.

[2] I.A. Viktorov, *Rayleigh and Lamb Waves* (Plenum Press, New York, 1967), pp. 93-96.

[3] L. Brekhovskikh and V. Goncharov, *Mechanics of Continua and Wave Dynamics* (Springer, New York, 1985), pp. 75-81. Note that the first of Eqs (5.16) has a sign error. The plus sign between the two terms should be replaced by a minus sign .

[4] Private communication.

[5] B.A. Auld, *Acoustic Fields and Waves in Solids*, Vol 2 (Krieger, Malabar, FL, 1990), pp.77-82.

[6] I.A. Viktorov, *Rayleigh and Lamb Waves* (Plenum Press, New York, 1967), p. 3.

Figure captions *Measurements of coupled Rayleigh wave propagation in an elastic plate* by Ti, O'Brien and Harris

Figure 1. The dispersion relation for the two lowest modes of an elastic plate. The upper curve is the symmetric mode and the lower the antisymmetric mode. The beatlength $L = \pi / \varepsilon$. Figure 2 indicates the particle displacement in the neighborhood of the intersections of the long dashed horizontal line with the dispersion curves.

Figure 2. A sketch of the x particle displacements corresponding to the neighborhoods of the intersection of the long dashed horizontal line in Fig. 1 with each dispersion curve. The solid lines indicate that the modes are in phase, while the dashed lines indicate that they are π out of phase. (a) symmetric mode; (b) antisymmetric mode; (c) algebraic sum of the two modes.

Figure 3. A sketch of the experimental arrangement viewed from above. The central axis of the focused transducer makes an angle θ_r with the vertical. The sound is coupled to the plate by means of a water-filled jacket. The plate is otherwise loaded only by the surrounding air. The focal point is placed at the plate surface and moved toward the stationary receiving transducer.

Figure 4. Representative data, case 4 of Table I. (a) The spatially amplitude-modulated, received signal plotted against position along the plate's surface (500 RMS data points, 100 *mm* scan distance). (b) The power spectrum of the signal from (a) plotted against the spatial frequency (1/distance). The vertical line indicates the theoretically estimated, spatial beat frequency.

Figure 5. A plot of $\omega h/c_t$ against L/h. The data points indicated by □ are the measured results. The data points indicated by ◆ are the theoretically predicted results. A ±10% error bar is attached to the theoretically estimated results.

Table captions ***Measurements of coupled Rayleigh wave propagation in an elastic plate*** by Ti, O'Brien and Harris

Table 1. The measured and calculated values of the important parameters. The temporal frequency f is the transducer operating frequency, f_a is the spatial frequency, L is the beatlength and h is the half-thickness of the brass plate. Note that case 4 is illustrated in Fig. 4.

Fig. 1 Ti, *et al.*

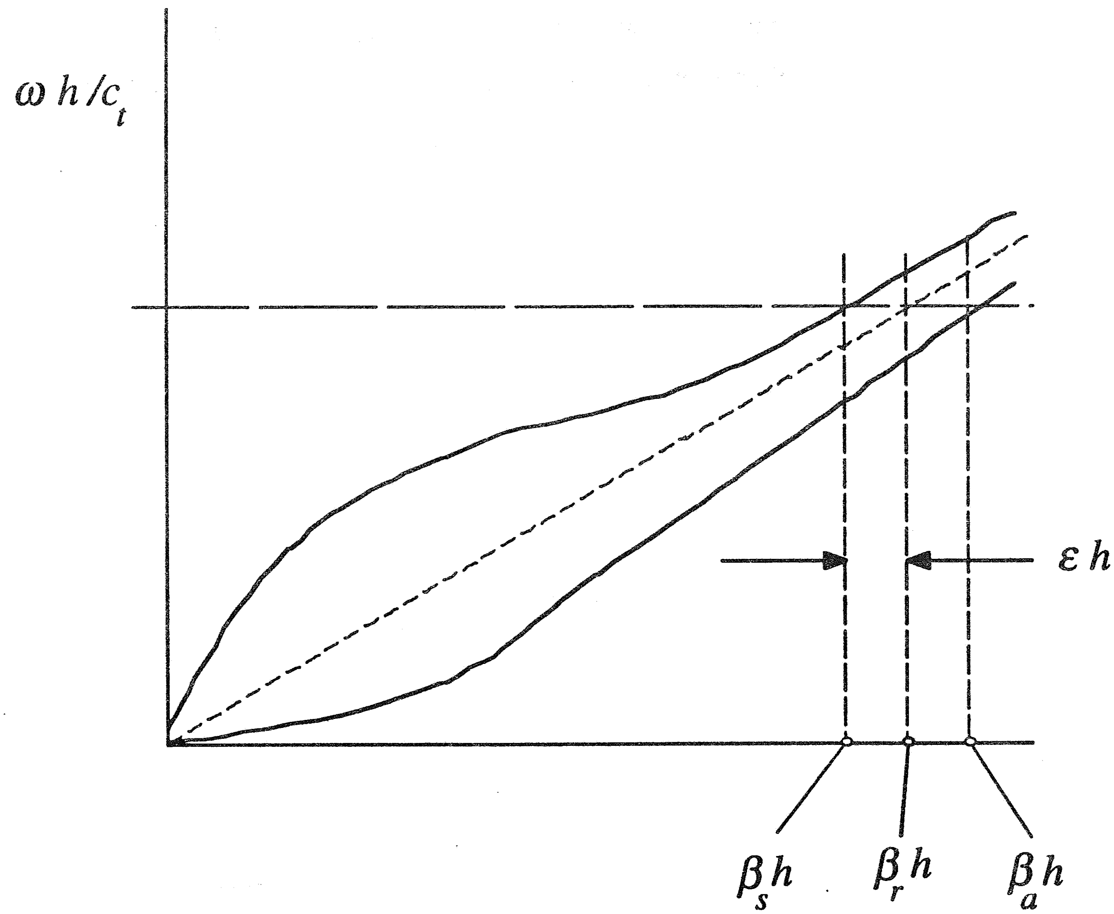

Fig.2 Ti, *et al.*

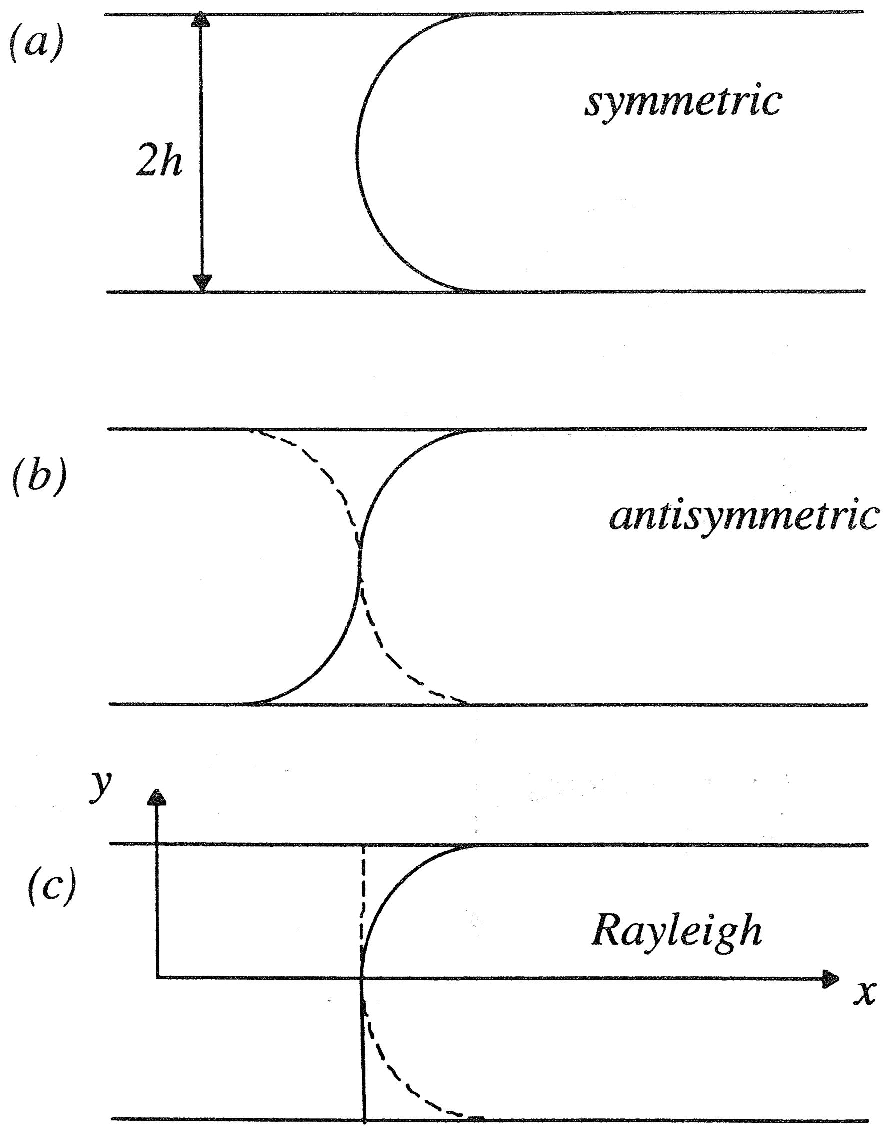

Fig. 3 Ti, *et al.*

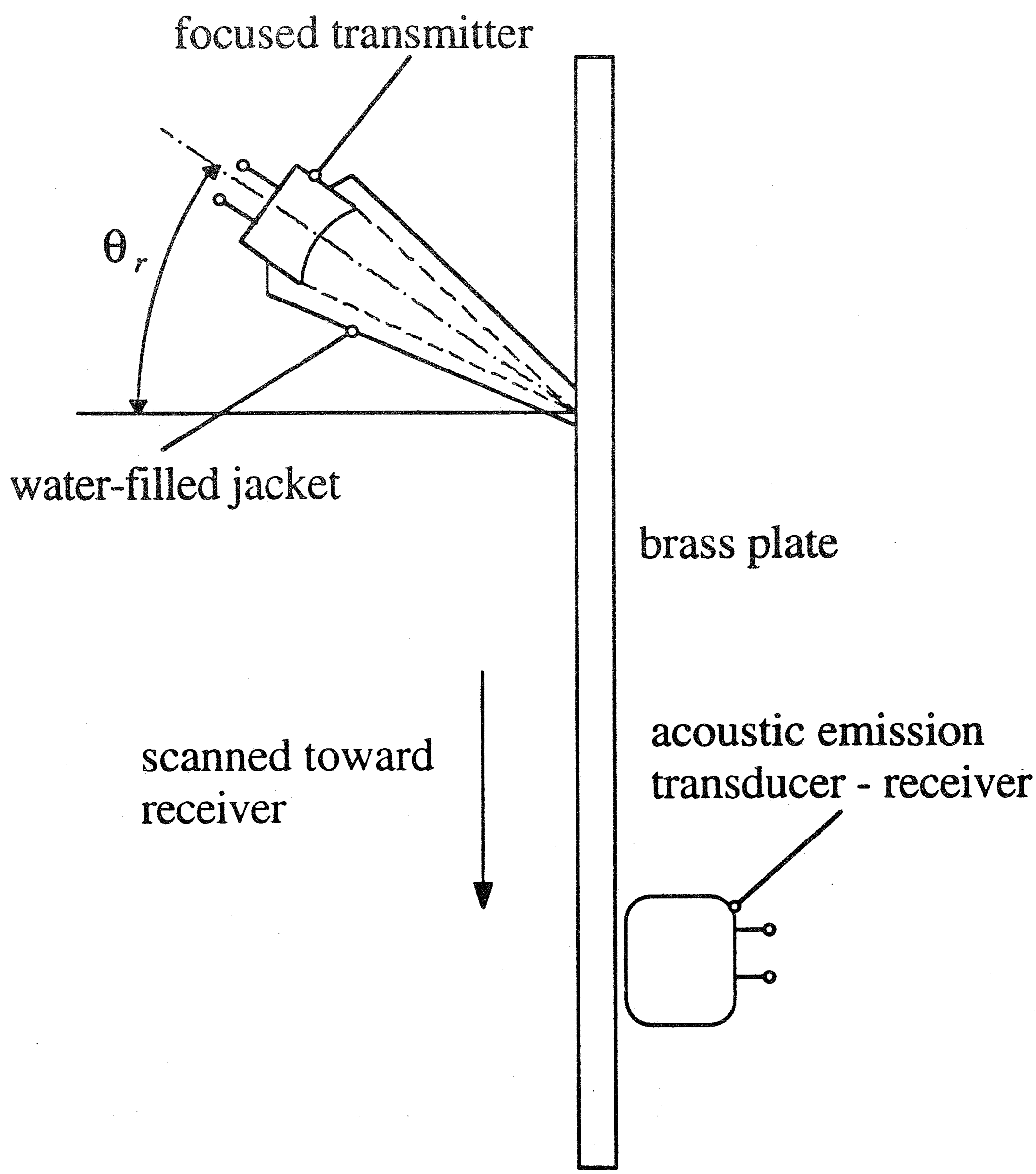
focused transmitter
θ_r
water-filled jacket
brass plate
scanned toward receiver
acoustic emission transducer - receiver

Fig. 4. Ti, *et al.*

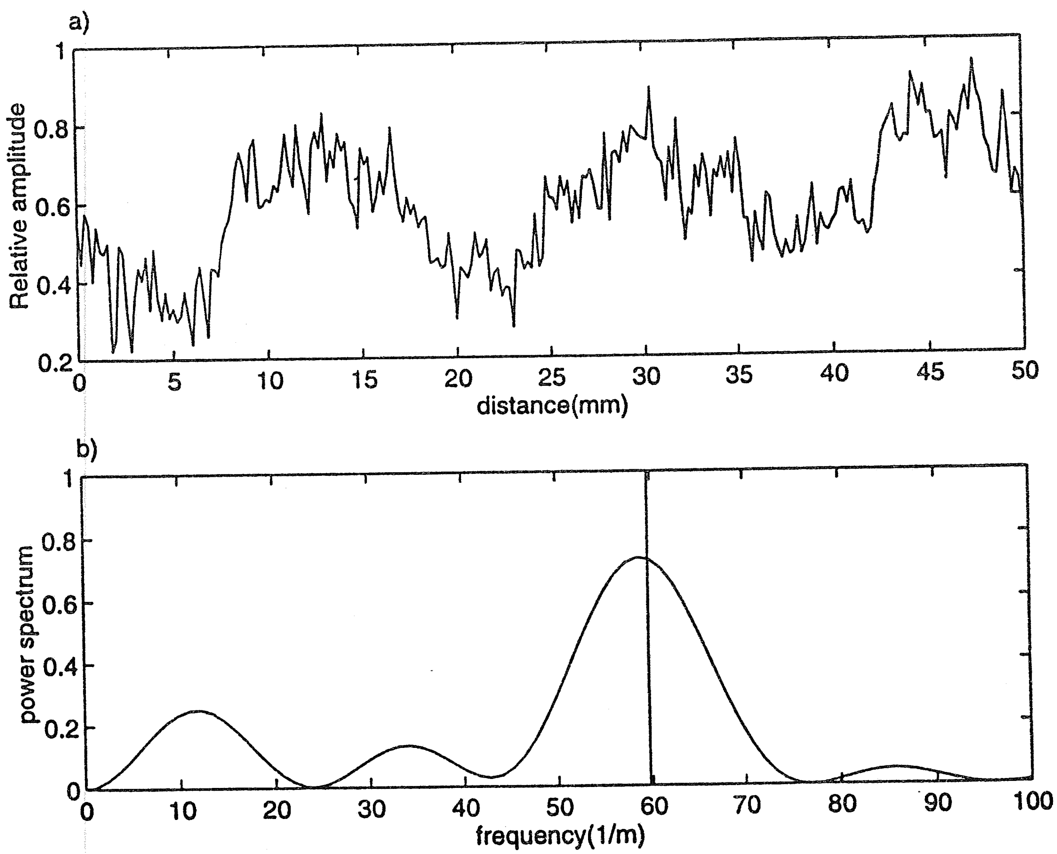
a)
Relative amplitude
1
0.8
0.6
0.4
0.2
0
5
10
15
20
25
30
35
40
45
50
distance(mm)
b)
power spectrum
1
0.8
0.6
0.4
0.2
0
0
10
20
30
40
50
60
70
80
90
100
frequency(1/m)

Fig. 5. Ti, *et al.*

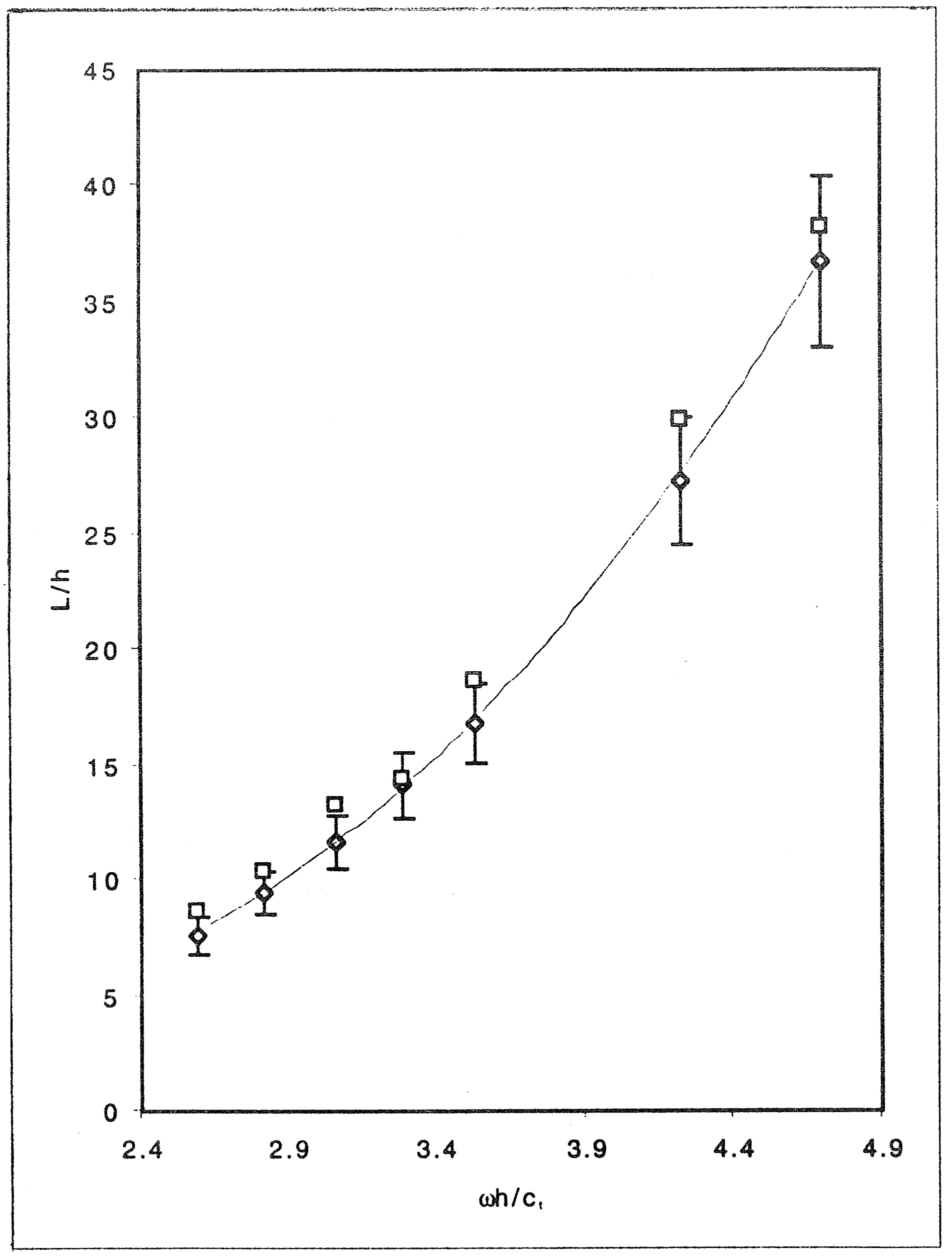

Table 1. Ti, *et al.*

				theory			experiment		
Case	f(MHz)	$\omega h/c_t$	β/ε	f_a (m^{-1})	L (mm)	L/h	f_a (m^{-1})	L (mm)	L/h
1	0.733	2.59	6.88	109.8	9.1	7.6	97.7	10.2	8.6
2	0.800	2.82	7.64	88.9	11.3	9.4	80.6	12.4	10.4
3	0.866	3.06	13.01	72.3	13.8	11.6	63.5	15.7	13.2
4	0.933	3.29	17.14	59.7	16.7	14.1	58.6	17.1	14.4
5	1.00	3.53	22.11	50.0	20.0	16.8	45.2	22.1	18.6
6	1.20	4.23	43.73	30.8	32.5	27.3	28.1	35.6	29.9
7	1.33	4.70	66.03	22.9	43.7	36.7	22.0	45.5	38.2

List of Recent TAM Reports

No.	Authors	Title	Date
752	Students in TAM 293–294	Thirty-first student symposium on engineering mechanics, J. W. Phillips, coordinator: Selected senior projects by D. N. Anderson, J. R. Dahlen, M. J. Danyluk, A. M. Dreyer, K. M. Durkin, J. J. Kriegsmann, J. T. McGonigle, and V. Tyagi	May 1994
753	Thoroddsen, S. T.	The failure of the Kolmogorov refined similarity hypothesis in fluid turbulence—*Physics of Fluids* **7**, 691–693 (1995)	May 1994
754	Turner, J. A., and R. L. Weaver	Time dependence of multiply scattered diffuse ultrasound in polycrystalline media—*Journal of the Acoustical Society of America* **97**, 2639–2644 (1995)	June 1994
755	Riahi, D. N.	Finite-amplitude thermal convection with spatially modulated boundary temperatures—*Proceedings of the Royal Society of London A* **449**, 459–478 (1995)	June 1994
756	Riahi, D. N.	Renormalization group analysis for stratified turbulence—*International Journal of Mathematics and Mathematical Sciences*, in press (1996)	June 1994
757	Riahi, D. N.	Wave-packet convection in a porous layer with boundary imperfections—*Journal of Fluid Mechanics* **318**, 107-128 (1996)	June 1994
758	Jog, C. S., and R. B. Haber	Stability of finite element models for distributed-parameter optimization and topology design—*Computer Methods in Applied Mechanics and Engineering*, in press (1996).	July 1994
759	Qi, Q., and G. J. Brereton	Mechanisms of removal of micron-sized particles by high-frequency ultrasonic waves—*IEEE Transactions on Ultrasonics, Ferroelectrics and Frequency Control* **42**, 619–629 (1995)	July 1994
760	Shawki, T. G.	On shear flow localization with traction-controlled boundaries—*International Journal of Solids and Structures* **32**, 2751–2778 (1995)	July 1994
761	Balachandar, S., D. A. Yuen, and D. M. Reuteler	High Rayleigh number convection at infinite Prandtl number with temperature-dependent viscosity	July 1994
762	Phillips, J. W.	Arthur Newell Talbot—Proceedings of a conference to honor TAM's first department head and his family	Aug. 1994
763	Man., C. S., and D. E. Carlson	On the traction problem of dead loading in linear elasticity with initial stress—*Archive for Rational Mechanics and Analysis* **128**, 223–247 (1994)	Aug. 1994
764	Zhang, Y., and R. L. Weaver	Leaky Rayleigh wave scattering from elastic media with random microstructures—*Journal of the Acoustical Society of America* **99**, 88-99 (1996)	Aug. 1994
765	Cortese, T. A., and S. Balachandar	High-performance spectral simulation of turbulent flows in massively parallel machines with distributed memory—*International Journal of Supercomputer Applications* **9**, 185–202 (1995)	Aug. 1994
766	Balachandar, S.	Signature of the transition zone in the tomographic results extracted through the eigenfunctions of the two-point correlation—*Geophysical Research Letters* **22**, 1941–1944 (1995)	Sept. 1994
767	Piomelli, U.	Large-eddy simulation of turbulent flows	Sept. 1994
768	Harris, J. G., D. A. Rebinsky, and G. R. Wickham	An integrated model of scattering from an imperfect interface—*Journal of the Acoustical Society of America* **99**, 1315-1325 (1996)	Sept. 1994
769	Hsia, K. J., and Z.-Q. Xu	The mathematical framework and an approximate solution of surface crack propagation under hydraulic pressure loading—*International Journal of Fracture*, in press (1996)	Sept. 1994
770	Balachandar, S.	Two-point correlation and its eigen-decomposition for optimal characterization of mantle convection	Oct. 1994
771	Lufrano, J. M., and P. Sofronis	Numerical analysis of the interaction of solute hydrogen atoms with the stress field of a crack—*International Journal of Solids and Structures*, in press (1996)	Oct. 1994
772	Aref, H., and S. W. Jones	Motion of a solid body through ideal fluid—Proceedings of the DCAMM 25th Anniversary Volume, 55-68 (1994)	Oct. 1994

List of Recent TAM Reports (cont'd)

No.	Authors	Title	Date
773	Stewart, D. S., T. D. Aslam, J. Yao, and J. B. Bdzil	Level-set techniques applied to unsteady detonation propagation—In "Modeling in Combustion Science," *Lecture Notes in Physics* (1995)	Oct. 1994
774	Mittal, R., and S. Balachandar	Effect of three-dimensionality on the lift and drag of circular and elliptic cylinders—*Physics of Fluids* **7**, 1841–1865 (1995)	Oct. 1994
775	Stewart, D. S., T. D. Aslam, and J. Yao	On the evolution of cellular detonation	Nov. 1994 *Revised* Jan. 1996
776	Aref, H.	On the equilibrium and stability of a row of point vortices—*Journal of Fluid Mechanics* **290**, 167–181 (1995)	Nov. 1994
777	Cherukuri, H. P., T. G. Shawki, and M. El-Raheb	An accurate finite-difference scheme for elastic wave propagation in a circular disk—*Journal of the Acoustical Society of America,* in press (1996)	Nov. 1994
778	Li, L., and N. R. Sottos	Improving hydrostatic performance of 1–3 piezocomposites—*Journal of Applied Physics* **77**, 4595–4603 (1995)	Dec. 1994
779	Phillips, J. W., D. L. de Camara, M. D. Lockwood, and W. C. C. Grebner	Strength of silicone breast implants—*Plastic and Reconstructive Surgery* **97**, 1215-1225 (1996)	Jan. 1995
780	Xin, Y.-B., K. J. Hsia, and D. A. Lange	Quantitative characterization of the fracture surface of silicon single crystals by confocal microscopy—*Journal of the American Ceramics Society* **78**, 3201-3208 (1995)	Jan. 1995
781	Yao, J., and D. S. Stewart	On the dynamics of multi-dimensional detonation—*Journal of Fluid Mechanics* **309**, 225-275 (1996)	Jan. 1995
782	Riahi, D. N., and T. L. Sayre	Effect of rotation on the structure of a convecting mushy layer—*Acta Mechanica* **118**, 109-120 (1996)	Feb. 1995
783	Batchelor, G. K., and TAM faculty and students	A conversation with Professor George K. Batchelor	Feb. 1995
784	Sayre, T. L., and D. N. Riahi	Effect of rotation on flow instabilities during solidification of a binary alloy—*International Journal of Engineering Science,* in press (1996)	Feb. 1995
785	Xin, Y.-B., and K. J. Hsia	A technique to generate straight surface cracks for studying the dislocation nucleation condition in brittle materials —*Acta Metallurgica et Materialia* **44**, 845-853 (1996).	Mar. 1995
786	Riahi, D. N.	Finite bandwidth, long wavelength convection with boundary imperfections: Near-resonant wavelength excitation—*International Journal of Mathematics and Mathematical Sciences,* in press (1996)	Mar. 1995
787	Turner, J. A., and R. L. Weaver	Average response of an infinite plate on a random foundation—*Journal of the Acoustical Society of America* **99**, 2167-2175 (1996)	Mar. 1995
788	Weaver, R. L., and D. Sornette	The range of spectral correlations in pseudointegrable systems: GOE statistics in a rectangular membrane with a point scatterer—*Physical Review E* **52**, 341 (1995)	Apr. 1995
789	Students in TAM 293–294	Thirty-second student symposium on engineering mechanics, J. W. Phillips, coordinator: Selected senior projects by K. F. Anderson, M. B. Bishop, B. C. Case, S. R. McFarlin, J. M. Nowakowski, D. W. Peterson, C. V. Robertson, and C. E. Tsoukatos	Apr. 1995
790	Figa, J., and C. J. Lawrence	Linear stability analysis of a gravity-driven Newtonian coating flow on a planar incline	May 1995
791	Figa, J., and C. J. Lawrence	Linear stability analysis of a gravity-driven viscosity-stratified Newtonian coating flow on a planar incline	May 1995
792	Cherukuri, H. P., and T. G. Shawki	On shear band nucleation and the finite propagation speed of thermal disturbances—*International Journal of Solids and Structures,* in press (1996)	May 1995

List of Recent TAM Reports (cont'd)

No.	*Authors*	*Title*	*Date*
793	Harris, J. G.	Modeling scanned acoustic imaging of defects at solid interfaces—Chapter in *IMA Workshop on Inverse Problems in Wave Propagation*, Springer-Verlag, in press (1996)	May 1995
794	Sottos, N. R., J. M. Ockers, and M. J. Swindeman	Thermoelastic properties of plain weave composites for multilayer circuit board applications	May 1995
795	Aref, H., and M. A. Stremler	On the motion of three point vortices in a periodic strip—*Journal of Fluid Mechanics* **314**, 1-25 (1996)	June 1995
796	Barenblatt, G. I., and N. Goldenfeld	Does fully-developed turbulence exist? Reynolds number independence versus asymptotic covariance—*Physics of Fluids* **7**, 3078–3082 (1995)	June 1995
797	Aslam, T. D., J. B. Bdzil, and D. S. Stewart	Level set methods applied to modeling detonation shock dynamics—*Journal of Computational Physics,* in press (1996)	June 1995
798	Nimmagadda, P. B. R., and P. Sofronis	The effect of interface slip and diffusion on the creep strength of fiber and particulate composite materials—*Mechanics of Materials*, in press (1996)	July 1995
799	Hsia, K. J., T.-L. Zhang, and D. F. Socie	Effect of crack surface morphology on the fracture behavior under mixed mode loading —*ASTM Special Technical Publication* 1296, in press (1996)	July 1995
800	Adrian, R. J.	Stochastic estimation of the structure of turbulent fields	Aug. 1995
801	Riahi, D. N.	Perturbation analysis and modeling for stratified turbulence	Aug. 1995
802	Thoroddsen, S. T.	Conditional sampling of dissipation in high Reynolds number turbulence—*Physics of Fluids* **8**, 1333-1335	Aug. 1995
803	Riahi, D. N.	On the structure of an unsteady convecting mushy layer—*Acta Mechanica*, in press (1996)	Aug. 1995
804	Meleshko, V. V.	Equilibrium of an elastic rectangle: The Mathieu–Inglis–Pickett solution revisited—*Journal of Elasticity* **40**, 207-238 (1995)	Aug. 1995
805	Jonnalagadda, K., G. E. Kline, and N. R. Sottos	Local displacements and load transfer in shape memory alloy composites	Aug. 1995
806	Nimmagadda, P. B. R., and P. Sofronis	On the calculation of the matrix–reinforcement interface diffusion coefficient in composite materials at high temperatures—*Acta Metallurgica et Materialia*, in press (1996)	Aug. 1995
807	Carlson, D. E., and D. A. Tortorelli	On hyperelasticity with internal constraints—*Journal of Elasticity* **42**, 91-98 (1966)	Aug. 1995
808	Sayre, T. L., and D. N. Riahi	Oscillatory instabilities of the liquid and mushy layers during solidification of alloys under rotational constraint—*Acta Mechanica*, in press (1996)	Sept. 1995
809	Xin, Y.-B., and K. J. Hsia	Simulation of the brittle-ductile transition in silicon single crystals using dislocation mechanics	Oct. 1995
810	Ulysse, P., and R. E. Johnson	A plane-strain upper-bound analysis of unsymmetrical single-hole and multi-hole extrusion processes	Oct. 1995
811	Fried, E.	Continua described by a microstructural field—*Zeitschrift für angewandte Mathematik und Physik*, in press (1996)	Nov. 1995
812	Mittal, R., and S. Balachandar	Autogeneration of three-dimensional vortical structures in the near wake of a circular cylinder	Nov. 1995
813	Segev, R., E. Fried, and G. de Botton	Force theory for multiphase bodies—*Journal of Geometry and Physics*, in press (1996)	Dec. 1995
814	Weaver, R. L.	The effect of an undamped finite-degree-of-freedom "fuzzy" substructure: Numerical solutions and theoretical discussion	Jan. 1996
815	Haber, R. B., C. S. Jog, and M. P. Bendsøe	A new approach to variable-topology shape design using a constraint on perimeter—*Structural Optimization* **11**, 1-12 (1996)	Feb. 1996
816	Xu, Z.-Q., and K. J. Hsia	A numerical solution of a surface crack under cyclic hydraulic pressure loading	Mar. 1996

List of Recent TAM Reports (cont'd)

No.	Authors	Title	Date
817	Adrian, R. J.	Bibliography of particle velocimetry using imaging methods: 1917–1995—*Produced and distributed in cooperation with TSI, Inc., St. Paul, Minn.*	Mar. 1996
818	Fried, E., and G. Grach	An order-parameter based theory as a regularization of a sharp-interface theory for solid–solid phase transitions—*Archive for Rational Mechanics and Analysis,* in press (1996)	Mar. 1996
819	Vonderwell, M. P., and D. N. Riahi	Resonant instability mode triads in the compressible boundary-layer flow over a swept wing	Mar. 1996
820	Short, M., and D. S. Stewart	Low-frequency two-dimensional linear instability of plane detonation	Mar. 1996
821	Casagranda, A., and P. Sofronis	On the scaling laws for the consolidation of nanocrystalline powder compacts	Apr. 1996
822	Xu, S., and D. S. Stewart	Deflagration-to-detonation transition in porous energetic materials: A comparative model study	Apr. 1996
823	Weaver, R. L.	Mean and mean-square responses of a prototypical master/fuzzy structure	Apr. 1996
824	Fried, E.	Correspondence between a phase-field theory and a sharp-interface theory for crystal growth—*Continuum Mechanics and Thermodynamics,* in press (1997)	Apr. 1996
825	Students in TAM 293–294	Thirty-third student symposium on engineering mechanics, J. W. Phillips, coordinator: Selected senior projects by W. J. Fortino II, A. A. Mordock, and M. R. Sawicki	May 1995
826	Riahi, D. N.	Effects of roughness on nonlinear stationary vortices in rotating disk flows—*Mathematical and Computer Modeling,* in press (1996)	June 1996
827	Riahi, D. N.	Nonlinear instabilities of shear flows over rough walls	June 1996
828	Weaver, R. L.	Multiple scattering theory for a plate with sprung masses: Mean and mean-square responses	July 1996
829	Moser, R. D., M. M. Rogers, and D. W. Ewing	Self-similarity of time-evolving plane wakes	July 1996
830	Lufrano, J. M., and P. Sofronis	Enhanced hydrogen concentrations ahead of rounded notches and cracks—Competition between plastic strain and hydrostatic constraint	July 1996
831	Riahi, D. N.	Effects of surface corrugation on primary instability modes in wall-bounded shear flows	Aug. 1996
832	Bechel, V. T., and N. R. Sottos	Measuring debond length in the fiber pushout test	Aug. 1996
833	Riahi, D. N.	Effect of centrifugal and Coriolis forces on chimney convection during alloy solidification	Sept. 1996
834	Cermelli, P., and E. Fried	The influence of inertia on configurational forces in a deformable solid—*Proceedings of the Royal Society of London A*, in press (1996)	Oct. 1996
835	Riahi, D. N.	On the stability of shear flows with combined temporal and spatial imperfections	Oct. 1996
836	Carranza, F. L., B. Fang, and R. B. Haber	An adaptive space–time finite element model for oxidation-driven fracture	Nov. 1996
837	Carranza, F. L., B. Fang, and R. B. Haber	A moving cohesive interface model for fracture in creeping materials	Nov. 1996
838	Balachandar, S., R. Mittal, and F. M. Najjar	Properties of the mean wake recirculation region in two-dimensional bluff body wakes	Dec. 1996
839	Ti, B. W., W. D. O'Brien, Jr., and J. G. Harris	Measurements of coupled Rayleigh wave propagation in an elastic plate	Dec. 1996